Evidence for Structural Symmetry and Functional Asymmetry in the Lactose Permease of *Escherichia coli*†

Aileen L. Green, Heather A. Hrodey, and Robert J. Brooker*

Department of Genetics, Cell Biology and Development, and the Biotechnology Institute, University of Minnesota, Minneapolis, Minnesota 55455

Received May 16, 2003; Revised Manuscript Received July 20, 2003

ABSTRACT: Previous work on the lactose permease of *Escherichia coli* has shown that mutations along a face of predicted transmembrane segment 8 (TMS-8) play a critical role in conformational changes associated with lactose transport (Green, A. L., and Brooker, R. J. [2001] *Biochemistry* 40, 12220−12229). Substitutions at positions 261, 265, 268, 272, and 276, which form a continuous stripe along TMS-8, were markedly defective for lactose transport velocity. In the current study, three single mutants (F261D, N272Y, N272L) and a double mutant (T265Y/M276Y) were chosen as parental strains for the isolation of mutants that restored transport function. A total of 68 independent mutants were isolated and sequenced. Forty-four were first-site revertants in which the original mutation was changed back to the wild-type residue or to a residue with a similar side-chain volume. The other 24 mutations were second-site suppressors in TMS-2 (Q60L, Q60P), loop 2/3 (L70H), TMS-7 (V229G/A), TMS-8 (F261L), and TMS-11 (F354V, C355G). On the basis of their locations, the majority of the second-site suppressors can be interpreted as improving the putative TMS-2/TMS-7/TMS-11 interface to compensate for conformational defects imposed by mutations in TMS-8 that disrupt the putative TMS-1/TMS-5/TMS-8 interface. Overall, this paper suggests that the TMS-2/TMS-7/TMS-11 interface is more important from a functional point of view, even though there is compelling evidence for structural symmetry between the two halves of the permease.

Integral membrane proteins, known as symporters, couple the uptake of cellular solutes with cation uptake (*1*, *2*). These transporters utilize the energy within ion electrochemical gradients to achieve active transport of the desired solute, which includes amino acids, metabolic intermediates, inorganic ions, and a variety of sugars. The lactose permease, located in the cytoplasmic membrane of *Escherichia coli*, has provided a model system to study the structure and function of symporters (*3*, *4*). The lactose permease couples the transport of H^+ and lactose with a 1:1 stoichiometry (*3*, *4*). The cloning and sequencing of the *lacY* gene has shown that the permease contains 417 amino acids and has a predicted molecular mass of 46 504 Da (*5*, *6*). Hydropathy plots, alkaline phosphatase fusions, suppressor analyses, and biophysical studies support a secondary model consisting of 12 transmembrane domains that cross the membrane as α-helices (*7*−*13*).

Several tertiary models for the lactose permease have been proposed (*14*−*17*). The models from our laboratory depict a tertiary arrangement in which the two halves of the protein form a rotationally symmetrical structure composed of six transmembrane domains each (*15*). We have hypothesized that conformational changes associated with lactose transport occur at the interface between the two halves of the permease (*18*, *19*). Recent crystallization studies of oxlT, an oxalate/formate antiporter that is homologous to the lactose permease, also suggest rotational symmetry between the two halves of the protein (*20*, *21*).

Evolutionarily, the lactose permease is a member of the major facilitator superfamily (MFS) that includes symporters, uniporters, and antiporters (*22*−*25*). Most members of the MFS are predicted to contain 12 membrane-spanning segments by hydrophobicity analysis (*14*). Among members of the superfamily, a general homology exists between the first and the second halves of the proteins, consistent with the hypothesis that the superfamily arose by a gene duplication/fusion event of a primordial gene encoding a protein of six transmembrane segments (*25*). A conserved decapeptide motif, G-X-X-X-D/E-R/K-X-G-R/K-R/K, is located in the loop that connects TMS-2 to TMS-3 and is repeated in the loop that connects TMS-8 to TMS-9 (*22*−*24*). The functional importance of amino acid residues within this motif has been extensively investigated in the lactose permease and tetracycline antiporter (*18*, *19*, *26*−*29*). While some minor differences are noted between these two proteins, the first position glycine and fifth position aspartate are critical for transport activity in the loop 2/3 motif (*18*, *26*). Individually, the basic residues within the lactose permease are not critical for transport function but may play a role in protein insertion and/or stability (*18*, *29*).

On the basis of the analysis of the conserved motif, our laboratory proposed that the general role of the decapeptide motif is to correctly position the interface between the two halves of the permease to facilitate conformational changes

† This work was supported by Grant GM53259 from the National Institutes of Health.

* To whom correspondence should be addressed. Tel.: (612) 624-3053. Fax: (612) 626-6140. E-mail: robert-b@biosci.umn.edu.

10.1021/bi034810+ CCC: $25.00
Published on Web 09/06/2003

associated with lactose transport (*28*, *29*). Accordingly, since our tertiary model predicts that TMS-2 and TMS-8 are located at this interface, extensive mutagenesis was conducted along these transmembrane segments (*15*, *30*). This work led to the identification of a stripe of residues in both transmembrane segments that is critical for transport velocity (*15*, *30*). Furthermore, an alignment of TMS-2 and TMS-8, created by matching the conserved loop 2/3 and conserved loop 8/9 motif, revealed a correspondence between the positions in TMS-2 and TMS-8 that comprise the critical face for conformational changes in each of these transmembrane segments (see ref *30* for a discussion). Taken together, these results suggest that the critical face of TMS-2 is located in a rotationally equivalent position to the critical face of TMS-8.

One approach that can yield useful information concerning the role of particular amino acid residues within proteins is an intragenic suppressor analysis. In this strategy, an amino acid of interest is mutated to a residue that impairs function, and then such a strain is used to isolate suppressor mutations that restore protein function. These can be first-site revertants in which the deleterious residue is replaced by a functional residue, or they can be second-site suppressor mutations in which an amino acid substitution somewhere else in the protein restores function. This type of approach has been previously conducted on the lactose permease and the tetracycline antiporter, starting with parental strains that had deleterious mutations in the loop 2/3 motif, TMS-2, or the loop 8/9 motif (*15*, *27*−*29*). The locations of the suppressor mutations suggest that their effect is to correct structural defects at the interface between the two halves of the permease that are caused by the first-site mutations. Many of these types of suppressors have been found in TMS-2, TMS-7, and TMS-11, suggesting that these helices are particularly important for conformational changes (*15*, *28*, *29*). Interestingly, these three transmembrane segments are located next to each other in our tertiary model, and it has been suggested from two laboratories that conformational changes associated with lactose transport may involve a scissoring motion of these transmembrane segments relative to each other (*15*, *31*, *32*).

In the current study, we began with parental strains containing inhibitory mutations in TMS-8. On the basis of our hypothetical tertiary model, this transmembrane segment is located at the critical interface between the two halves of the permease and is located opposite from the region of the protein containing TMS-2/TMS-7/TMS-11 (see Figure 1). We report the results of the isolation of 68 independent mutations.

MATERIALS AND METHODS

Reagents. Lactose (*O*-*β*-D-galactopyranosyl-(1,4)-α-D-glucopyranose) and melibiose (*O*-α-D-galactopyranosyl-(1,6)-α-D-glucopyranose) were purchased from Sigma Chemical Co., St. Louis, MO. [^{14}C]-Lactose and sequenase (version 2.0) were purchased from Amersham Pharmacia Biotech. Restriction enzymes and DNA ligase were purchased from New England BioLabs, Inc. (Beverly, MA). All remaining reagents were of analytical grade.

Bacterial Strains and Methods. The relevant genotypes of the bacterial strains and plasmids are described in Table 1. Plasmid DNA was purified using the Eppendorf Plasmid Mini DNA Kit (Westbury, NY). Restriction digests and ligations were performed according to the manufacturers' recommendations. Cell cultures were grown in YT media (*33*) supplemented with tetracycline (0.01 mg/mL).

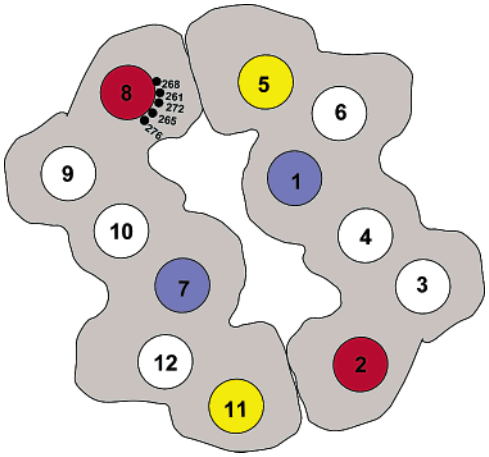

FIGURE 1: Cross-sectional model of the lactose permease. The basic features of this model were originally described in ref *14*, and a revised model that incorporated recent cross-linking and biophysical data was proposed in ref *15*. The overall shape of the permease is meant to emphasize the concept of rotational symmetry. For example, helix-1 in the first half of the permease is equivalent to helix-7 in the second half.

In Vitro Galactoside Transport. HS4006/F′I^{Q}Z^{+}Y^{-} cells containing plasmids carrying the wild-type or mutant permeases were grown at 37 °C with shaking to mid-log phase in YT media supplemented with 0.005 mg/mL of tetracycline and 0.25 mM isopropylthiogalactoside (IPTG). The cells were collected by centrifugation at 5000*g* for 5 min. The cell pellet was washed in phosphate buffer, pH 7.0, containing 60 mM K_2HPO_4 and 40 mM KH_2PO_4, and then resuspended in the same buffer at a concentration of 0.5 mg of protein/mL. In a standard assay, the cells were equilibrated at 30 °C for 5−10 min before [^{14}C]-lactose (1.0 μCi/mL) was added to a final concentration of 0.1 mM. Aliquots of 200 μL were removed at the appropriate time points (15 s, 30 s, and 1 min), and the cells were captured on 0.45 μm Metricel membranes (Gelman Sciences, Inc., Ann Arbor, MI). The assay was linear for 1 min or longer. The cells were then washed with 5−10 mL of ice-cold phosphate buffer by rapid filtration. The filter with the cells was then placed in liquid scintillation fluid and counted using a Beckman LS1801 liquid scintillation counter. The HS4006/F′I^{Q}Z^{+}Y^{-} strain carrying the pAlter-1 vector with no *lacY* insert was used to determine the background level of lactose transport. This background value was subtracted from the experimental values to determine the nmoles of [^{14}C]-lactose taken up per mg of total cellular protein. Uphill and downhill transport assays were similar except that a *lacZ* minus strain was used in the uphill assays. In these assays, lactose accumulation appeared to plateau in the wild-type and mutant strains after a three-minute incubation.

DNA Sequencing. Following identification of suppressor strains with a red phenotype on melibiose MacConkey plates, double-stranded plasmid DNA was sequenced according to Kraft et al. (*34*). The entire coding sequence of each gene was sequenced.

Table 1: Bacterial Strains and Plasmids

strain[a]	Relevant Genotype chromosome/F′/plasmid	ref
T184	*lacI*$^+$ *lacO*$^+$ *lacZ*$^-$ *lacY*$^-$/ *lacI*^{Q} lacO$^+$ *lacZU*^{118} (*lacY*$^+$)/−	*47*
HS4006/F′I^{Q}Z$^+$Y$^-$	Δ(*lac-pro*)Δ*malB101*/ *lacI*^{Q} *lacO*$^+$ *lacZ*$^+$ *lacY*$^-$/−	*48*
pAlterLacY[b]	−/−/Δ(*lacI*) *lacO*$^+$Δ(*lacZ*) *lacY*$^+$ Δ(*lacA*) *Tet*^{R}	*30*

strain[c]	level of protein expression % WT ± SE
wild-type	100
parental strains	
F261D	152 ± 39[d]
N272L	92 ± 35
N272Y	67 ± 20[d]
T265Y/M276Y	121 ± 14[d]
first-site revertant strains	
D261Y	83 ± 20
Y272N	100
Y272D	46 ± 3
Y272S	40 ± 2
L272V	70 ± 2
Y265S/M276Y	6 ± 9
Y265C/M276Y	110 ± 16
second-site suppressor strains	
N272L/Q60L	75 ± 24
N272L/V229G	68 ± 25
N272L/V229A	37 ± 2
N272L/F354V	30 ± 5
T265Y/M276Y/F261L	164 ± 9
T265Y/M276Y/Q60P	195 ± 48
T265Y/M276Y/L70H	388 ± 4
T265Y/M276Y/C355G	258 ± 19

[a] In strain T184, *lacZ*^{U118} is a polar nonsense mutation, which results in a *LacZ*$^-$*LacY*$^-$ phenotype (*47*). [b] pAlterLacY was constructed by cloning the 2300-bp EcoRI fragment from pLac184 (*49*), which carries the wild-type *lacY* gene, into the EcoRI site of pAlter-1 (accession number X65334). The *lacY* gene and the tetracycline resistance gene are in the opposite transcriptional direction. [c] Expression levels were measured in strain T184 containing the plasmid with a wild-type *lacY* gene (pAlter-LacY) or a *lacY* gene with the designated mutation(s). [d] Measured in ref *30*.

Membrane Isolation and Western Blot Analysis. A total of 10 mL of mid-log cells grown as for transport assays were collected by centrifugation (5000*g*, 10 min). The pellet was quickly frozen in liquid nitrogen and resuspended in 800 μL of MTPBS (150 mM NaCl, 16 mM Na_2HPO_4, 4 mM NaH_2PO_4) plus phenylmethylsulfonyl fluoride (0.1 mg/mL) and pepstatin A (1 μg/mL). The suspension was quickly frozen two more times in liquid nitrogen and then sonicated three times for 20 s each. Triton X-100 was added to a final concentration of 1%, and the membrane fraction was collected by centrifugation. The pellet was resuspended in 100 μL of MTPBS and subjected to a modified Lowry protein assay (Sigma). A sample of 100 μg of protein was subjected to SDS−polyacrylamide gel electrophoresis on a 12% acrylamide gel. The proteins were electroblotted to nitrocellulose, and Western blot analysis was performed according to Sambrook et al. (*35*). The primary polyclonal antibody recognizes the lactose permease C-terminal 10 amino acids. The secondary antibody, goat-anti-rabbit, conjugated to alkaline phosphatase was purchased from Sigma. The Western blot was then scanned using a Molecular Dynamics laser densitometer and analyzed by comparison to wild-type values for the same preparation and Western blot. The values are reported as a percentage of wild-type for three separate preparations.

Table 2: Locations of Revertant and Suppressor Mutations

secondary parent strain[a]	mutation	number of isolates	location in secondary structural model[a]
first-site revertants			
F261D	D261Y	20	TMS-8
N272Y	Y272N	10	TMS-8
N272Y	Y272D	5	TMS-8
N272Y	Y272S	1	TMS-8
N272L	L272V	1	TMS-8
T265Y/M276Y	Y265S	3	TMS-8
T265Y/M276Y	Y265C	4	TMS-8
second-site suppressors			
N272L	Q60L	3	TMS-2
N272L	V229G	4	TMS-7
N272L	V229A	5	TMS-7
N272L	F354V	4	TMS-11
T265Y/M276Y	F261L	2	TMS-8
T265Y/M276Y	Q60P	3	TMS-2
T265Y/M276Y	L70H	1	Loop 2/3
T265Y/M276Y	C355G	2	TMS-11

[a] Based on the secondary model described in ref *30*.

RESULTS

Isolation of Suppressor Mutants. In a previous study, mutagenesis was conducted along the side of predicted TMS-8 that contains the first amino acid in the conserved loop 8/9 motif (*30*). Several substitutions at positions 261, 265, 268, 272, and 276 were markedly defective for downhill lactose transport although these mutants were well-expressed. According to helical wheel plots, Phe-261, Thr-265, Gly-268, Asn-272, and Met-276 form a continuous stripe along one face of TMS-8. In our tertiary model, these residues face toward TMS-5 and TMS-1 (see Figure 1). Several strains involving mutations at these positions were severely defective and formed white colonies on melibiose MacConkey plates. This phenotype indicates that these strains are unable to transport melibiose, an α-galactoside that is transported very well by the wild-type lactose permease.

For the current study, three strains (F261D, N272Y, N272L) and a double mutant (T265Y/M276Y) were chosen as parental strains for the isolation of suppressor mutations. As shown in Table 1, these strains were expressed at normal levels. With the exception of the N272Y mutation, the codon changes in these mutations were designed in such a way that a single base change could not restore the wild-type codon. When streaked on MacConkey plates containing 0.4 or 1% melibiose, these strains formed white colonies. After a few days, however, suppressor mutations were identified as red flecks in the primary streak. These red flecks were restreaked to isolate individual red colonies and to confirm that the mutation suppressed the white phenotype of the parental strain.

As shown in Table 2, a total of 68 mutants were saved and subjected to DNA sequencing. Some of the red mutants were first-site revertants in which the mutant codon was changed to a residue that increased activity. In the case of the F261D parental strain, 20 independent isolates were sequenced, and all were first-site revertants to tyrosine. The codon change was a transversion mutation in which a purine was changed to a pyrimidine in the first nucleotide of the codon (GAT to TAT). In the case of the N272Y parental

strain, 10 of the isolates were first-site revertants in which the codon was changed back to wild-type (Y272N). The other six isolates were first-site revertants to aspartic acid or serine. Again, the mutations involved a single transversion mutation at one nucleotide position within the codon: Y272N (TAT to AAT), Y272D (TAT to GAT), and Y272S (TAT to TCT). The first-site revertants did not seem to exert their effects by altering expression levels because the parental strains and first-site revertants all showed moderate to high levels of expression, within the range of the wild-type permease (Table 1). Instead, a common feature of the first-site revertants was that their side-chain volume closely approximated the side-chain volume of the wild-type residue. At position 261, the wild-type phenylalanine residue has a side-chain volume of 191.9 A^3, based on the average volume of buried residues in proteins whose volumes are not affected by ligand binding (*36*). This volume is much higher than the buried volume of aspartic acid (117.3 $Å^3$) but similar to that of tyrosine (197.0 $Å^3$). Likewise, the wild-type residue at position 272, which is asparagine, has a buried volume of 124.7 $Å^3$. A leucine residue found at position 272 in the inactive parental strain has a buried side-chain volume of 164.0 $Å^3$, whereas the first-site revertants were smaller. Valine, serine, and aspartic acid have buried volumes of 139.0, 95.4, and 117.3 $Å^3$, respectively. With regard to the T265Y/M276Y parental strain, revertants occurred only at position 265. The wild-type threonine residue has a volume of 121.5 $Å^3$, while the inhibitory tyrosine substitution has a volume of 197.0 $Å^3$. The serine and cysteine revertants would have side-chain volumes of 95.4 and 103.3 $Å^3$, respectively. Thus, the effect was to decrease side-chain volume.

The second-site suppressors fell into two categories. One of the suppressors, F261L, is on the same face of TMS-8 as the original parental mutations, T265Y/M276Y. Presumably, this mutation restores the proper topology of TMS-8 within the lactose permease. However, the other suppressors found at positions 60, 70, 229, 354, and 355 are seen to cluster in the TMS-2, TMS-7, TMS-11 region. According to our tertiary model, these three transmembrane segments are adjacent to each other but not near TMS-8 (see Figure 1). All TMS-2 second-site suppressors were found at position 60. This position was identified in previous work as being part of a critical face of TMS-2 that is important for conformational changes (*15*). The Q60P mutation would place a kink in the middle of TMS-2, while the Q60L suppressor would substitute a bulkier side chain. The loop 2/3 suppressor, L70H, is located at the seventh position of the conserved loop 2/3 motif. While the seventh position is not highly conserved, the suppressor adds a basic residue to the motif that is immediately adjacent to the highly conserved eighth position glycine. This suppressor may exert its effects by altering the loop 2/3 motif in such a way as to affect the topology of TMS-2 and/or TMS-3. Finally, suppressors in TMS-7 and TMS-11 were identified that decreased side-chain volume. In TMS-7, Val-229 was changed to alanine or glycine. In TMS-11, Phe-354 was changed to valine or Cys-355 was changed to glycine.

Phenotype on MacConkey Plates. To initially examine the effects of the suppressor mutations, the wild-type, parent, and suppressor strains were screened for their phenotype on MacConkey indicator plates (Table 3). These plates contained lactose (a β-galactoside) or melibiose (an α-galactoside) at two different concentrations: 0.4 and 1.0%. A strain exhibiting good transport of these sugars will have a red phenotype. Strains having intermediate levels of transport will show a pink phenotype, while a white phenotype indicates very low transport activity. As expected, the wild-type strain is red on lactose and melibiose plates, while the parental strains have a white or pink phenotype. All of the suppressors have a red or pink phenotype on melibiose MacConkey plates. This is expected since these plates were originally used to identify the suppressor mutations. In addition, most of the suppressors also showed a red or pink phenotype on lactose MacConkey plates as well. Even so, several suppressors showed a significant preference of melibiose over lactose. These include the Y272D, L272V, N272L/V229A, and N272L/F354V strains. Interestingly, all of these strains involved a mutation at position 272, suggesting that mutations at this site may alter sugar specificity in a way that favors the α-galactoside over the β-galactoside.

Table 3: Phenotype on MacConkey Plates[b]

	melibiose		lactose	
strain[a]	0.4%	1.0%	0.4%	1.0%
wild-type	red	red	red	red
parental strains				
F261D	pink	pink	white	white
N272Y	white	white	white	white
N272L	pink	pink	white	white
T265Y/M276Y	pink	pink	white	white
first-site revertants				
D261Y	red	red	red	red
Y272N	red	red	red	red
Y272D	pink	pink	white	white
Y272S	red	red	red	red
L272V	red	red	pink	pink
Y265S/M276Y	red	red	red	red
Y265C/M276Y	red	red	red	red
second-site suppressors				
N272L/Q60L	red	red	pink	pink
N272L/V229G	red	red	red	red
N272L/V229A	red	red	pink	pink
N272L/F354V	red	red	white	white
T265Y/M276Y/F261L	red	red	white	pink
T265Y/M276Y/Q60P	red	red	red	red
T265Y/M276Y/L70H	red	red	red	red
T265Y/M276Y/C355G	red	red	white	white

[a] The designated plasmids were transformed into *E. coli* strain HS4006/F′$I^QZ^+Y^-$. [b] The transformed strains were streaked onto MacConkey plates containing the designated sugar concentration, and the color of colonies was observed the following day.

Downhill Lactose Transport. To examine lactose transport quantitatively, the wild-type and mutant strains were assayed for their ability to transport [^{14}C]-lactose. Table 4 compares transport results of the wild-type, parental strains, and the suppressors in which lactose transport was assayed in a *lacZ* positive strain so that lactose is rapidly metabolized upon entry into the cell. This is termed a downhill assay since lactose moves down its concentration gradient (*37*). As expected, the wild-type strain transports lactose at a relatively rapid rate. In contrast, all of the parental strains are severely defective for downhill transport. The first-site revertants at positions 261 and 272 show moderate transport, while the first-site revertants at position 265 show low but detectable levels of transport.

Likewise, there was variation in the downhill transport rates of the suppressor strains. Suppressors of the N272L

Table 4: Quantitative Measurement of Lactose Transport

strain	downhill initial rate[a] (percentage of wild-type)	uphill lactose accumulation (in/out)[b]
pAlterLacY (wild-type)	100 ± 8.3	46.4 ± 3.0
parental strains		
F261D	<0.1	0.1 ± 0.1
N272L	1.2 ± 0.1	1.0 ± 0.2
N272Y	0.2 ± 0.1	1.5 ± 0.4
T265Y/M276Y	<0.1	0.2 ± 0.2
first-site revertants		
D261Y	43.4 ± 7.9	39.8 ± 0.8
Y272N	N. D.	N. D.
Y272D	21.3 ± 2.4	16.2 ± 3.2
Y272S	6.4 ± 2.3	5.0 ± 0.2
L272V	2.4 ± 0.1	2.3 ± 0.2
Y265S/M276Y	2.3 ± 0.1	3.3 ± 0.5
Y265C/M276Y	2.2 ± 0.2	0.8 ± 0.1
second-site suppressors		
N272L/Q60L	7.5 ± 0.6	7.4 ± 3.2
N272L/V229G	24.1 ± 0.1	7.4 ± 1.4
N272L/V229A	2.1 ± 0.3	4.6 ± 0.6
N272L/F354V	3.0 ± 0.2	2.8 ± 0.4
T265Y/M276Y/F261L	2.2 ± 0.1	1.1 ± 0.3
T265Y/M276Y/Q60P	2.2 ± 0.2	2.5 ± 0.5
T265Y/M276Y/L70H	0.6 ± 0.1	3.4 ± 0.8
T265Y/M276Y/C355G	0.9 ± 0.2	1.1 ± 0.4

[a] Initial rates of downhill lactose transport were measured in strain HS4006/F′$I^{Q}Z^{+}Y^{-}$ carrying the wild-type or designated mutant plasmids as described under Materials and Methods using 0.1 mM final lactose concentration. [b] Steady-state level of accumulation of lactose at 3 min was measured in strain T184 carrying the wild-type or designated mutant plasmids as described under Materials and Methods at an external lactose concentration of 0.1 mM.

mutation tended to have higher activity as compared to suppressors of the double mutant (T265Y/M276Y); however, the latter suppressors showed transport levels that were higher than the parental strain. Taken together, the downhill transport data indicate that the first-site revertants and second-site suppressors restore transport function, but to varying degrees. In general, the transport velocities in the parent and suppressor strains correlated reasonably well with the MacConkey phenotypes, with a few exceptions. The Y265S/M276Y, Y265C/M276Y, T265Y/M276Y/Q60P, and T265Y/M276Y/L70H strains were red on lactose MacConkey plates, yet had relatively low rates of transport. Since the MacConkey plates have a much higher concentration of sugar as compared to the transport assay, these mutants may have a poor affinity for lactose but a moderate velocity for transport. Alternatively, the D261Y strain had a high rate of lactose transport at a low sugar concentration yet was white on MacConkey plates. This result could be explained by a high affinity for sugar coupled with a somewhat poor velocity. It is also possible that the rates of transport are influenced by differences (e.g., pH, buffer, etc.) in the transport assay as compared with the growth on plates.

Uphill Lactose Transport. Another important aspect of lactose permease function is the ability to effectively couple the transport of H^+ with lactose. This enables the cells to accumulate lactose against a concentration gradient, using the proton electrochemical gradient as the driving force for uphill sugar transport. Table 4 compares transport results of the wild-type, parental strains, and the suppressors. As expected, the wild-type strain accumulates lactose to a high intracellular/extracellular ratio of approximately 45. In contrast, all of the parental strains are defective for uphill accumulation. As a general trend, the suppressors exhibited higher levels of accumulation as compared with their respective parental strains. The first-site revertants at positions 261 and 272 showed moderate to high levels of accumulation. The D261Y strain accumulated lactose to levels that were similar to the wild-type strain, while the Y272D, Y272S, and L272V strains showed a more moderate level of accumulation. By comparison, the first-site revertants at position 265 showed low but detectable levels of accumulation.

A similar trend in accumulation is seen among the second-site suppressors. Those suppressors that are coupled with the N272L mutation exhibited moderate levels of accumulation. As seen in Table 4, these strains can accumulate lactose in a range of 2−7-fold higher than the extracellular medium. The suppressors coupled to the T265Y/M276Y mutations, however, only showed low levels of accumulation. These fell in the 1−4-fold range of accumulation. Overall, the results seen in Table 4 indicate that the suppressors substantially restore the ability to accumulate lactose against a concentration gradient. However, the ability of the suppressor mutations to restore accumulation is severely limited in strains containing mutations at positions 265 and 276. These results parallel the effects of the mutations on downhill lactose transport.

DISCUSSION

A suppressor analysis can provide a myriad of information regarding protein structure and function. First-site revertants can give insights regarding the features of an amino acid residue that are important for protein function. As mentioned earlier, the first-site revertants obtained in this study suggest that side-chain volume at positions 261, 265, and 272 is important to maintain the proper topology of TMS-8 (see Table 2). This work supports our conclusions obtained in a previous study, which indicated that a face on TMS-8 containing Gly-268, Phe-261, Asn-272, Thr-265, and Met-276 plays a critical role in lactose transport activity. In that earlier work, mutations at these codons, which involved significant changes in side-chain volume, had detrimental effects on the initial rate of downhill transport, the maximal velocity of transport, and the uphill accumulation of lactose (*30*).

In the current study, second-site suppressors were also obtained. In some cases, second-site suppressors may provide clues regarding structural proximity between two regions of a protein. A first-site mutation may disrupt secondary or tertiary structure, and the suppressor mutation may restore the defect in structure. In such a scenario, the suppressor mutation may be near the first-site mutation in the secondary or tertiary structure of the protein and restore topology. Alternatively, suppressors may not be immediately adjacent to the imposed defect but may globally affect protein structure in a way that compensates for the first-site defect. As a third possibility, a suppressor may not directly restore the structural impairment caused by the first-site mutation but may compensate for its effect functionally. For example, two regions of a protein may be important for its activity. A mutation that causes a defect in one region may be functionally compensated by mutations in the other region that substantially improve activity.

To judge whether the second-site suppressors obtained in this study exert their effects due to structural proximity or functional compensation, it is important to consider the arrangement of α-helices in tertiary models of the lactose permease. Models from our laboratory and another laboratory place TMS-8 in close proximity to TMS-5 (*14*−*17*). This information is based on bioinformatics, cross-linking, site-directed chemical cleavage, and site-directed spin labeling studies (*38*−*40*). In other work, the face of TMS-8 juxtaposed to TMS-5 included several residues (Val-264, Gly-268, and Asn-272) sensitive to cysteine replacement that displayed substrate protection against inactivation and labeling by *N*-ethylmaleimide (*41*). The authors of that study concluded that the face of TMS-8 with Val-264, Gly-268, and Asn-272 is in close proximity to the substrate recognition site, which is believed to contain Cys-148 (TMS-5). Using site-directed excimer fluorescence and site-directed spin labeling of A273C and M299C, Wang et al. (*42*) demonstrated proximity of TMS-8 to transmembrane segment 9 (TMS-9). Proximity has also been shown between TMS-8 and TMS-9 by engineering divalent metal binding sites (bis-His residues) with the construction of a R302H/E269H/H322F mutant (*13*). Finally, residue pairs of Glu-269 and His-322 in TMS-10 have been placed near each other based upon site-directed excimer fluorescence and engineered metal-binding sites (*43*, *44*). The results of these studies indicated that the face of TMS-8 containing the negatively charged residue (Glu-269) is close to the positively charged residues on TMS-9 and TMS-10. Suppressor analysis involving neutral residues at positions 269 and 319 has also suggested proximity between TMS-8 and TMS-10 (*45*). Overall, current tertiary models agree on the proximity of TMS-8 to TMS-5, TMS-9, and TMS-10 (*14*−*17*). In addition, cross-linking data suggest proximity between TMS-8 and TMS-7 (*40*). However, due to the relatively long length of the cross-linker, it is equivocal whether TMS-7 and TMS-8 are adjacent in the tertiary structure of the permease. Our model (see Figure 1) suggests that they are within close proximity (not immediately adjacent), while the tertiary model from another laboratory suggests that they are adjacent with a gap in between (*14*−*17*).

An analysis of oxlT, another member of MFS, suggests that TMS-7 and TMS-8 are not adjacent (*46*). Indeed, a structural model for that protein based on a 6.5 Å resolution structure combined with biochemical and other biophysical data is in agreement with our model shown in Figure 1. The major difference is that our simplified model depicts the transmembrane segments as running parallel, while more detailed data in oxlT indicate that many transmembrane segments are not entirely perpendicular to the plane of the lipid bilayer. Nevertheless, the oxlT model shows TMS-2 interacting with TMS-11 and TMS-5 interacting with TMS-8 at the interface between the two halves of the protein. Furthermore, TMS-7 is in direct proximity to TMS-2 and TMS-11, while TMS-1 is in direct proximity to TMS-5 and TMS-8. Therefore, the idea that TMS-2/TMS-7/TMS-11 on one side of the protein and TMS-1/TMS-5/TMS-8 on the other side of the protein form important structural interactions is supported by the genetic analyses of the lactose permease described in Table 5 as well as structural studies concerning oxlT.

Table 5: Occurrence of Suppressor Mutations in the TMS-1/5/8 or 2/7/11 Region[a]

first-site mutation(s)	location in 2° structure[b]	second-site suppressor[b]	location in 2° structure
TMS-1/5/8 Region			
Q60V	TMS-2	Y26H	TMS-1
G64C/S/V	loop 2/3	P28S/L/T	TMS-1
G64S	loop 2/3	F29S	TMS-1
G64C	loop 2/3	C154G	TMS-5
T265Y/M276Y	TMS-8	F261L	TMS-8
G64S	loop 2/3	F261V	TMS-8
TMS-2/7/11 Region			
D68S	loop 2/3	T45R	TMS-2
P280L	loop 8/9	G46C/S	TMS-2
P280L	loop 8/9	F49L	TMS-2
G64S	loop 2/3	A50T	TMS-2
P280L	loop 8/9	A50T	TMS-2
Q60A/V	TMS-2	S53F/Y	TMS-2
Q60A	TMS-2	S56L	TMS-2
S56L/Q	TMS-2	Q60L/P	TMS-2
N272L	TMS-8	Q60L	TMS-2
T265Y/M276Y	TMS-8	Q60P	TMS-2
T265Y/M276Y	TMS-8	L70H	loop 2/3
P280L	loop 8/9	L212Q	loop 6/7
P280L	loop 8/9	L216Q	loop 6/7
S56Q/L	TMS-2	V229G/A	TMS-7
N272L	TMS-8	V229G/A	TMS-7
P280L	loop 8/9	S233P	TMS-7
D68S/T	loop 2/3	C234W	TMS-7
G64C/S	loop 2/3	C234F	TMS-7
G64S	loop 2/3	Q241L	TMS-7
D68S/T	loop 2/3	F247V	TMS-7
D68T	loop 2/3	G257D	loop 7/8
N272L	TMS-8	F354V	TMS-11
P280L	loop 8/9	F354C/V	TMS-11
T265Y/M276Y	TMS-8	C355G	TMS-11
Q60A	TMS-2	Q359L	TMS-11
D68S	loop 2/3	S366F	TMS-11
G64S	loop 2/3	V367E	TMS-11
D68S	loop 2/3	V367E	TMS-11
G64V	loop 2/3	A369P	TMS-11
D68T	loop 2/3	A369P	TMS-11
P280L	loop 8/9	G370C/S/V	TMS-11

[a] Second-site suppressors of loop 2/3, TMS-2, and loop 8/9 mutations were identified in previous studies (*15*, *18*, *28*, *50*). The second-site suppressors of TMS-8 mutations are described in this paper (see Table 2). [b] The location of suppressors is based on a secondary structural model described previously (*30*). In addition to the suppressors described in this table, one suppressor was not located in either region: C333G (TMS-10).

On the basis of tertiary models and the previous work just described, it is concluded that most of the second-site suppressors obtained in the current study are not in close proximity to the first-site mutations that they correct. An exception would be the F261L suppressor located in TMS-8 (see Table 2). In that case, the suppressor is located on the same face of TMS-8 as the parent mutation. It is reasonable to speculate that the F261L mutation exerts its effects by restoring the proper topology of TMS-8. With regard to suppressor mutations in TMS-7 (i.e., V229G and V229A), it is unclear whether they exert a direct structural effect on TMS-8 due to conflicts among recent tertiary models and ambiguity in cross-linking data. However, it should be pointed out that identical suppressors at position 229 were also obtained in suppressor screens involving first-site mutations in TMS-2 (*15*). On the basis of tertiary models and the available biochemical data discussed previously, it would be difficult to see how position 229 mutations could be structurally adjacent to both TMS-2 and TMS-8. Instead,

it seems more likely that the mutations at position 229 functionally complement the defect in TMS-8 by altering the structure of a distant region of the permease. Likewise, the suppressors obtained at positions 60, 70, 354, and 355 could be interpreted in this manner. Since TMS-2 and TMS-8 are not predicted to be close to each other in any tertiary model, it seems more likely that they exert their effects by functionally complementing the defect caused by mutations in TMS-8 rather than directly restoring the proper topology to TMS-8 per se.

On the basis of the ideas just discussed, a central question rests on the underlying effects of first-site mutations on lactose permease function. How do first-site mutations in TMS-8 affect permease function? According to a helical wheel plot of TMS-8, codons 261, 265, 268, 272, and 276 form a continuous stripe on TMS-8 (see Figure 1). These residues are on the same side of TMS-8 as Pro-280, which is the first amino acid in the conserved loop 8/9 motif. Previous studies have shown that Pro-280 is important for conformational changes associated with lactose transport. Large side-chain volume substitutions (P280Y, P280M, and P280L) at this position are inhibitory to transport function (*19*). Likewise, bulky substitutions within TMS-8 on the same face as Pro-280 significantly reduce the maximal velocity of lactose transport (*30*). The results of these two studies indicate that this face of TMS-8 is important for the putative conformational changes necessary for lactose transport. Thus, first-site mutations are expected to exert their effects by inhibiting conformational changes. If such conformational changes only involved TMS-8, the suppressors a priori could only correct the defect by restoring TMS-8 topology. However, we have proposed that conformational changes involving H^+/lactose transport are far more complex. Specifically, our earlier work has suggested that the critical conformational changes occur at the interface between the two halves of the permease and involves two regions: the TMS-1/TMS-5/TMS-8 region and the TMS-2/TMS-7/TMS-11 region. We previously suggested that a putative conformational change involves TMS-2 sliding against TMS-11 and TMS-7 in a scissoring motion (*15*). This suggestion was supported by cross-linking data in the presence and absence of sugar (*31*, *32*) and by suppressor analysis (*15*, *18*, *28*). Furthermore, based upon the rotational symmetry of our tertiary model and the cross-linking studies that have been performed thus far, which show close interaction between TMS-8 and TMS-5, we also proposed a similar movement of the helices at the other interface between the two halves of the protein (*30*). In one conformation, TMS-8 may be relatively parallel to TMS-5, while in the other conformation TMS-8 would lie obliquely across TMS-1 and TMS-5. During the putative conformational changes, this critical face of TMS-8 may interact with residues in TMS-5 and TMS-1.

Except for the F261L mutation, the second-site suppressors obtained in the current work can be interpreted as improving the TMS-2/TMS-7/TMS-11 interface to compensate for conformational defects imposed by mutations at the TMS-1/TMS-5/TMS-8 interface (i.e., mutations in TMS-8). Along these lines, the work from many studies, both in the lactose permease and tetracycline antiporter, suggests that the TMS-2/TMS-7/TMS-11 interface is more important from a functional point of view. Indeed, in both transporters, mutations in the loop 2/3 motif are much more inhibitory as compared with analogous mutations in the loop 8/9 motif (*18*, *19*, *26*, *27*). Likewise, an extensive array of suppressor analyses, including the one described here, suggests that the TMS-2/TMS-7/TMS-11 interface is more important for function. Table 5 summarizes the locations of second-site suppressor mutations that have been obtained from parental strains harboring inhibitory mutations in TMS-2, loop 2/3, TMS-8, or loop 8/9 in the lactose permease. As seen here, significantly more second-site suppressors have been found in the TMS-2/TMS-7/TMS-11 region as compared with the TMS-1/TMS-5/TMS-8 region. Mutations at five positions in the TMS-1/TMS-5/TMS-8 region can correct first-site mutations in TMS-2, loop 2/3, TMS-8, or loop 8/9, while 19 mutations in the TMS-2/TMS-7/TMS-11 region can restore activity. As seen in Table 5, second-site suppressor mutations were obtained along much of the length of TMS-2 (codon 45 to 60), TMS-7 (codon 229 to 247), and TMS-11 (codon 354 to 370). In contrast, only a few sites in TMS-1, TMS-5, or TMS-8 were able to suppress first-site defects. Taken together, the data suggest that the TMS-2/TMS-7/TMS-11 region is either more critical from a functional point of view and/or more sensitive to mutations that affect the ability of the permease to make necessary conformational changes associated with lactose transport. Therefore, a significant functional asymmetry appears to exist between the two halves of the permease.

Despite the aforementioned functional asymmetry, the argument for structural symmetry is quite compelling. Indeed, as originally noted by Maiden et al., the gene sequence of MFS members has arisen from a primordial gene encoding a protein having six transmembrane segments. During evolution, this gene has duplicated and fused to create the modern MFS gene encoding a protein with 12 transmembrane segments (ref *25*, also see ref *24* for a review). This observation alone would strongly predict that the first and second halves of MFS proteins would have very similar folding patterns. Likewise, a bioinformatic analysis of many members of the MFS showed that the two halves of MFS proteins are very similar with regard to the lengths of hydrophilic loops and the amphipathicity of transmembrane segments (*14*). In addition, structural symmetry is suggested from suppressor analyses involving the mirror substitutions in the two halves of the lactose permease. As seen in Table 5, spontaneous second-site suppressor mutations in similar or identical regions of the permease were obtained from two independent parental strains containing first-site mutations at analogous positions in either half of the permease. For example, an A50T mutation was seen to correct a loop 2/3 and a loop 8/9 defect, and V229G/A suppressors could correct TMS-2 and TMS-8 defects. It should be emphasized that the suppressor mutations are mutations that arise spontaneously, not the result of site-directed mutagenesis. Structural symmetry is also consistent with previous mutagenesis work along TMS-8 (*30*). In that study, an alignment of TMS-2 and TMS-8 created by matching the conserved loop 2/3 and conserved loop 8/9 motif showed a striking overlap between the critical positions in TMS-2 and TMS-8. Finally, crystallographic work of oxlT, a member of the MFS, is consistent with symmetry. The crystallographic arrangement of the transmembrane regions of oxlT closely match the tertiary models we have proposed for the lactose

permease (*20*, *21*). Taken together, a large body of experimental data supports the idea that the members of MFS exhibit rotational symmetry. Moreover, analogous codons in TMS-2 and TMS-8 appear to represent critical positions along each transmembrane segment where putative conformational changes take place. The overlap of codons within the critical face of TMS-2 and TMS-8, along with the biophysical and biochemical studies placing these codons in domains of interaction with TMS-11 and TMS-5, respectively, support the primary feature of our tertiary model of the lactose permease, rotational symmetry.

ACKNOWLEDGMENT

We would like to thank Dr. Thomas H. Wilson for providing us with the antibody used in the experiment of Table 1 and Mr. Ethan Anderson for his assistance with the protein expression experiments.

REFERENCES

1. Mitchell, P. (1963) *Biochem. Soc. Symp. 22*, 142−168.
2. Crane, R. K. (1977) *Rev. Physiol. Biochem. Pharmacol. 78*, 99−159.
3. West, I. C., and Mitchell, P. (1973) *Biochem. J. 132*, 587−592.
4. West, I. C. (1970) *Biochem. Biophys. Res. Commun. 41*, 655−661.
5. Teather, R. M., Muller-Hill, B., Abrutsch, U., Aichele, G., and Overath, P. (1978) *Mol. Gen. Genet. 159*, 239−248.
6. Buchel, D. E., Gronenborg, B., and Muller-Hill, B. (1980) *Nature 283*, 541−545.
7. Foster, D. L., Boublik, M., and Kaback, H. R. (1983) *J. Biol. Chem. 258*, 31−34.
8. Calamia, J., and Manoil, C. (1990) *Proc. Natl. Acad. Sci. U.S.A. 87*, 4937−4941.
9. Calamia, J., and Manoil, C. (1992) *J. Mol. Biol. 224*, 539−543.
10. King, S. C., Hansen, C. L., and Wilson, T. H. (1991) *Biochim. Biophys. Acta 1062*, 177−186.
11. Patzlaff, J. S., Moeller, J. A., Barry, B. A., and Brooker, R. J. (1998) *Biochemistry 37*, 15363−15375.
12. Carrasco, N., Tahara, S. M., Patel, L., Goldkorn, T., and Kaback, H. R. (1982) *Proc. Natl. Acad. Sci. U.S.A. 79*, 6894−6898.
13. He, M. M., Voss, J., Hubbell, W. L., and Kaback, H. R. (1997) *Biochemistry 36*, 13682−13687.
14. Goswitz, V. C., and Brooker, R. J. (1995) *Protein Sci. 4*, 534−537.
15. Green, A. L., Anderson, E. J., and Brooker, R. J. (2000) *J. Biol. Chem. 275*, 23240−23246.
16. Kaback, H. R., Voss, J., and Wu, J. (1997) *Curr. Opin. Struct. Biol. 7*, 537−542.
17. Kaback, H. R., Sahin-Toth, M., Weinglass, A. B. (2001) *Nature Rev. Mol. Cell Biol. 2*, 610−620.
18. Jessen-Marshall, A. E., and Brooker, R. J. (1996) *J. Biol. Chem. 271*, 1400−1404.
19. Pazdernik, N. J., Jessen-Marshall, A. E., and Brooker, R. J. (1997) *J. Bacteriol. 179*, 735−741.
20. Heymann, J. A., Sarker, R., Hirai, T., Shi, D., Milne, J. L., Maloney, P. C., and Subramaniam, S. (2001) *EMBO J. 20*, 4408−4413.
21. Hirai, T., Heymann, J. A., Shi, D., Sarker, R., Maloney, P. C., and Subramaniam, S. (2002) *Nat. Struct. Biol. 9*, 597−600.
22. Griffith, J. K., Baker, M. E., Rouch, D. A., Page, M. G. P., Skurray, R. A., Paulsen, I. T., Chater, K. F., Baldwin, S. A., and Henderson, P. F. J. (1992) *Curr. Opin. Cell Biol. 4*, 684−695.
23. Henderson, P. J. F. (1990*) J. Bioenerg. Biomembr. 22*, 525−569.
24. Pao, S. S., Paulsen, I. T., and Saier, M. J., Jr. (1998) *Microbiol. Mol. Biol. Rev. 62*, 1−34.
25. Maiden, M. C. J., Davis, E. O., Baldwin, S. A., Moore, D. C. M., and Henderson, P. J. F. (1987) *Nature 325*, 641−643.
26. Yamaguchi, A., Someya, Yl., and Sawai, T. (1992) *J. Biol. Chem. 267*, 19155−19162.
27. Yamaguchi, A., Inagaki, Y., and Sawai, T. (1995) *Biochemistry 34*, 11800−11806.
28. Jessen-Marshall, A. E., Parker, N. J., and Brooker, R. J. (1997) *J. Bacteriol. 179*, 2616−2622.
29. Pazdernik, N. J., Matzke, E. A., Jessen-Marshall, A. E., and Brooker, R. J. (2000) *J. Membr. Biol. 174*, 31−40.
30. Green, A. L., and Brooker, R. J. (2001) *Biochemistry 40*, 12220−12229.
31. Wu, H., Hardy, D., and Kaback, H. R. (1998) *J. Mol. Biol. 282*, 959−967.
32. Wu, H., and Kaback, H. R. (1997) *J. Mol. Biol. 270*, 285−293.
33. Miller, J. (1972) *Experiments in Molecular Genetics*, p 433, Cold Spring Harbor Laboratory, Cold Spring Harbor, NY.
34. Kraft, R., Tardiff, J., Drauter, K. S., and Leinwand, L. A. (1988) *Biotechniques 6*, 544−547.
35. Sambrook, J., Fritsch, E. F., and Maniatas, T. (1989) *Molecular Cloning: A Laboratory Manual*, Cold Spring Harbor Laboratory, Cold Spring Harbor, NY.
36. Tsai, J., Taylor, R., Chothia, C., and Gerstein, M. (1999) *J. Mol. Biol. 290*, 253−266.
37. Rickenberg, H. V., Cohen, G., Buttin, G., and Monod, J. (1956) *Ann. Inst. Pasteur (Paris) 91*, 829−857.
38. Wu, J., Hardy, D., and Kaback, H. R. (1999) *Biochemistry 38*, 2320−2325.
39. Wu, J., Perrin, D. M., Sigman, D. S., and Kaback, H. R. (1995) *Proc. Natl. Acad. Sci. U.S.A. 92*, 9186−9190.
40. Wu, J., Voss, J., Hubbell, W. L., and Kaback, H. R. (1996) *Proc. Natl. Acad. Sci. U.S.A. 93*, 10123−10127.
41. Frillingos, S., and Kaback, H. R. (1997) *Protein Sci. 6*, 438−443.
42. Wang, Q., Voss, J., Hubbell, W. L., and Kaback, H. R. (1998) *Biochemistry 37*, 4910−4915.
43. Jung, K., Jung, H., Wu, J., Prive, G. G., and Kaback, H. R. (1993) *Biochemistry 32*, 12273−12278.
44. Jung, K., Voss, J., He, M., Hubbell, W. L., and Kaback, H. R. (1995) *Biochemistry 34*, 6272−6277.
45. Lee, J., Hwang, P. P., and Wilson, T. H. (1993) *J. Biol. Chem. 268*, 20007−20015.
46. Hirai, T., Heymann, J. A., Maloney, P. C., and Subramaniam, S. (2003) *J. Bacteriol. 185*, 1712−1718.
47. Teather, R. M., Bramhall, J., Riede, I., Wright, J. K., Furst, M., Aichele, G., Wilhelm, U., and Overath, P. (1980) *Eur. J. Biochem. 108*, 223−231.
48. Brooker, R. J., and Wilson, T. H. (1985) *Proc. Natl. Acad. Sci. U.S.A. 82*, 3959−3963.
49. Franco, P. J., and Brooker, R. J. (1994) *J. Biol. Chem. 269*, 7379−7386.
50. Pazdernik, N. J., Cain, S. M., and Brooker, R. J. (1997) *J. Biol. Chem. 272*, 26110−26116.

BI034810+